Two scattering experiments were carried out where the circular polarization of the 0.845-Mev γ ray was investigated. The results of these experiments are given in Fig. 8. The counting rate of the temperature monitor counter $W(\theta=90°)$ is given together with the counting rate in the Compton-scattering peak (energy range 0.54–0.72 Mev, see Fig. 5) from the incident γ ray, giving $W(\theta=15°)$. The effect E, defined in Eq. (6), is given in the lowest curve of Fig. 8. We find that the effect as defined above is $E=+(0.040\pm0.005)$ at the lowest temperatures; thus the counting rates in the scattering counter are larger, when the polarizing field H_p and the analyzing field H_a are opposite in direction, than in the case of the fields in the same direction. From the analysis of the angular momenta in the decay of Mn^{56}, the sign of the hyperfine coupling constant of the Mn ions (see, for instance, Trenam[19]), and the sign of the circular-polarization-dependent part of the Compton scattering cross section, we get a positive magnetic moment for Mn^{56}.

It is found that the circular polarization effect in Mn^{56} drops faster than the anisotropy of the angular distribution of the γ rays. This is thought to be due to the magnetic hfs level sequence of Mn in cerium magnesium nitrate, where nuclear magnetic substates m_I of opposite sign (from different fine-structure groups m_S) have a level spacing of the same order of magnitude as the magnetic substates m_I within one level group m_S.

ACKNOWLEDGMENTS

Acknowledgment is made to the U. S. Air Force for use of the Laboratory for Nuclear Science Data Center which was established with funds provided by the Air Force Office of Scientific Research under a contract.

We wish to express our appreciation to Professor W. M. Whitney for his advice during the course of our low-temperature experiments; to Mr. Earle F. White for the cyclotron bombardments; to Mrs. Elizabeth W. Backofen for the chemical separations; and to Mr. David S. Baker for help in data-taking during the latter stages of this experiment.

PHYSICAL REVIEW VOLUME 117, NUMBER 2 JANUARY 15, 1960

Alpha-Alpha Scattering in the Energy Range 5 to 9 Mev*

C. M. Jones, G. C. Phillips, and Philip D. Miller†
The Rice Institute, Houston, Texas
(Received August 13, 1959)

The scattering of alpha particles from helium has been experimentally studied in the energy range 5 to 9 Mev by the measurement of three excitation functions at the center-of-mass angles 30° 33′, 54° 44′, and 70° 7′. A phase-shift analysis has been performed which indicates that only the S- and D-wave phase shifts are necessary to fit the data in this energy region. Only the well-known D state at approximately 2.9 Mev in Be^8 was observed. The D state has been compared to the single-level dispersion theory and level parameters have been extracted which are compatible with the alpha-particle model of Be^8.

INTRODUCTION

THE scattering of alpha particles by helium has been studied for many years. The first alpha-alpha scattering experiment was reported by Rutherford and Chadwick in 1927,[1] and their work was repeated and extended by other investigators. This early work was summarized in 1941, by Wheeler.[2] Unfortunately, the accuracy of these early experiments was limited by the necessity of using natural alpha-particle sources. The most recent, and precise alpha-alpha scattering experiments have been performed by Heydenburg and Temmer[3] at the Carnegie Institution in the energy range of 0.15 to 3 Mev; by Russell, Phillips, and Reich[4] at the Rice Institute in the energy range 2.5 to 5.5 Mev; by Nilson, Jentschke, Briggs, Kerman, and Snyder[5,6] at the Univeristy of Illinois in the energy range 12 to 23 Mev; and by Burcham *et al.*[7] at the University of Birmingham in the energy range 23 to 38.4 Mev.

Phase-shift analyses have been performed on all of these recent data and it is found that the only nonzero phase shifts needed to fit the data to a laboratory energy of 35 Mev are those corresponding to $l=0$, 2, 4, 6, and 8. Furthermore, only three states are observed

* Supported in part by the U. S. Atomic Energy Commission.
† Now at Oak Ridge National Laboratory, Oak Ridge, Tennessee.
[1] E. Rutherford and J. Chadwick, Phil. Mag. **4**, 605 (1927).
[2] J. A. Wheeler, Phys. Rev. **59**, 16 (1941).
[3] N. P. Heydenburg and G. M. Temmer, Phys. Rev. **104**, 123 (1956).
[4] Russell, Phillips, and Reich, Phys. Rev. **104**, 135 (1956).
[5] Nilson, Jentschke, Briggs, Kerman, and Snyder, Phys. Rev. **104**, 1673 (1956).
[6] Nilson, Jentschke, Briggs, and Kerman, Phys. Rev. **109**, 846 (1958).
[7] Burcham, McKee, Gibson, Bredin, Evans, Prowse, and Rotblat, *Comptes Rendus du Congres International de Physique Nucléaire Interactions Nucléaires aux Basses Energies et Structure des Noyaux*, Paris, 1958, edited by P. Guggenberger (Dunod, Paris, 1959).

in the compound nucleus Be^8 in this energy range; a narrow 0^+ ground state at approximately 190-kev bombarding energy, a broad 2^+ state at approximately 2.9 Mev in Be^8, and an even broader 4^+ state at approximately 11 Mev in Be^8. Since the alpha particle is a Bose-Einstein particle, it is impossible to observe states in Be^8 of either odd angular momentum or odd parity through alpha-alpha scattering. However, there is no evidence from the study of the reactions $Li^6(He^3,p)Be^8$,[8] $Li^7(d,n)Be^8$,[9] $B^{11}(p,He^4)Be^8$,[10] and $B^{10}(d,He^4)Be^8$ [10] for the presence of other states in Be^8 in the energy regions from 0 to 12 Mev.

In the present experiment the work of Russell, Phillips, and Reich has been extended to 9 Mev using the He^{4++} beam from the Rice Institute 5.5-Mev Van de Graaff accelerator. Phase shifts have been extracted and the 2.9-Mev state has been studied using the single-level dispersion theory. No new states in Be^8 were observed.

EXPERIMENTAL DATA

The large volume scattering chamber used in the present experiment has been described in detail by Russell *et al.*[4]

The data presented in this paper consists of three excitation curves measured in the energy range 5 to 9 Mev. The center-of-mass angles chosen for these excitation curves were 30° 33′, 54° 44′, and 70° 7′. These angles were chosen because the first and third are zeros of the fourth Legendre polynominal and the second is a zero of the second Legendre polynominal. These excitation curves are shown in Fig. 1. Also shown in Fig. 1 are points representing the fit from the phase-shift analysis. The present data are also shown in Fig. 2 with the data of Heydenburg and Temmer, Russell *et al.*, and Nilson *et al.* Smooth curves have been arbitrarily drawn through the data points in this figure.

The estimated rms errors in the data due to geometry, detection efficiency, and current integration are 3.3% for the 30° 33′ data, and 2.9% for the 54° 44′ and 70° 7′ data. Due to the necessity of using the weak doubly charged alpha beam the statistical errors in the data are rather high. In particular, the lowest point in the minimum of the 70° 7′ curve near 5 Mev has a statistical error of 17%. However, with the exception of the seven points near this minimum the 70° 7′ data have a statistical error of less than 3%. The 54° 44′ data have a statistical error which ranges from 2% at 5 Mev to 7% at 9 Mev. The statistical error in the 30° 33′ data varies from 0.8% at 5 Mev to 0.3% at 7 Mev.

The energy scale was established by performing a $Li^7(p,n)Be^7$ neutron threshold experiment using the HH^+ beam from the Van de Graaff accelerator with the same geometry as was used in the scattering experiment. The threshold energy for this reaction was taken as 1.8814 Mev.[11] The bombarding energy is estimated to be accurately known to within 20 kev.

PHASE-SHIFT ANALYSIS

The first step taken in the analysis of the data was the extraction of experimental nuclear phase shifts. The center-of-mass cross section $\sigma_{c.m.}(\theta)$ can be expressed[12] in terms of the nuclear phase shifts δ_l by

$$\sigma_{c.m.}(\theta)=|-(\eta/2k)\csc^2[\theta/2]\exp\{i\eta\ln\csc^2(\theta/2)\}$$
$$-(\eta/2k)\csc^2[\pi/2-\theta/2]$$
$$\times\exp\{i\eta\ln\csc^2[\pi/2-\theta/2]\}$$
$$+2/k\sum_{l=0,2,4,\cdots}(2l+1)\sin\delta_l P_l(\cos\theta)$$
$$\times\exp[i\alpha_l+i\delta_l]|^2,$$

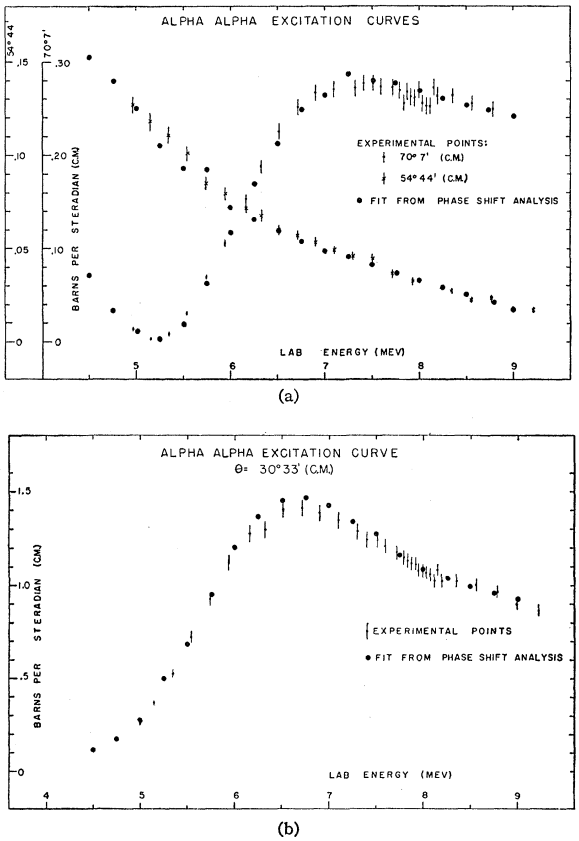

FIG. 1. Alpha-alpha scattering center-of-mass cross sections at the center-of-mass angles 30°33′, 54°44′, and 70°7′ plotted as a function of laboratory energy. The fit from the phase-shift analysis is also shown in the form of closed circles.

[8] C. D. Moak and W. R. Wisseman, Phys. Rev. **101**, 1326 (1956).
[9] C. C. Trial and C. H. Johnson, Phys. Rev. **95**, 1363 (1954).
[10] Holland, Inglis, Malm, and Mooring, Phys. Rev. **99**, 92 (1955).
[11] Jones, Douglas, McEllistrem, and Richards, Phys. Rev. **94**, 947 (1954).
[12] L. I. Schiff, *Quantum Mechanics* (McGraw-Hill Book Company, Inc., New York, 1955).

where

$$\eta=4e^2/hv, \quad \alpha_l=2\sum_{s=1}^{l}\tan^{-1}(\eta/s), \quad \alpha_0=0.$$

Here k is the wave number, v is the velocity of the incident alpha particles, θ is the center-of-mass scattering angle, and $P_l(\cos\theta)$ is the Legendre polynomial of order l.

The phase shifts were extracted in the following manner. It was first assumed, on the basis of previous experiments, that the data could be fit with only δ_0, δ_2, δ_4. An IBM-650 digital computer was then programmed to calculate $\sigma_{\text{c.m.}}(\theta)$ at a given energy for the three scattering angles used in the experiment. Assumed trial values of these three phase shifts were employed. The computer then found an error function, $\sum E$, defined by

$$\sum E=\sum_{\theta}\frac{1}{\nu_\theta}\left(\frac{\sigma_{\text{ex}}(\theta)-\sigma_{\text{cal}}(\theta)}{\sigma_{\text{ex}}(\theta)}\right)^2,$$

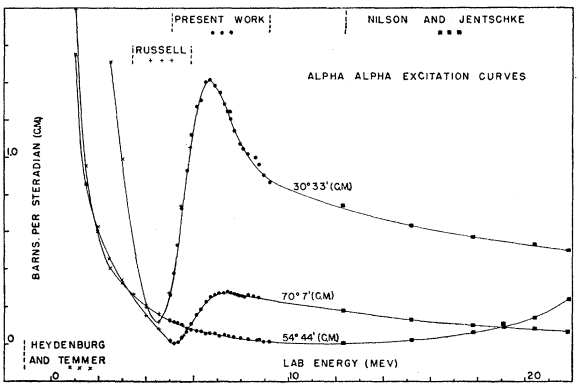

FIG. 2. Alpha-alpha scattering center-of-mass cross sections plotted *versus* the laboratory energy. Data from the present work at the center-of-mass angles 30°33′, 54°44′, and 70°7′ are shown along with data points of Heydenburg and Temmer, Russell *et al.*, and Nilson *et al.* Arbitrary curves have been drawn through the data points.

where $\sigma_{\text{ex}}(\theta)$ is the center-of-mass experimental cross section, $\sigma_{\text{cal}}(\theta)$ is the center-of-mass calculated cross section, and ν_θ is a confidence factor. The computer then minimized this error function by successive computation of the $\sigma_{\text{cal}}(\theta)$ with different values of δ_0, δ_2, and δ_4. The $\sigma(\theta)$ computation part of the program was checked with an accurate hand calculation, while the minimizing logic was checked by means of several graphical solutions.

The program was first run with $\nu_\theta=1$ for all θ's and energies. It was found that the phase shift fits to the excitation curves were in general good except near the maximum of the 30° 33′ and 70° 7′ curves. This difficulty was rectified by adjusting the ν's so as to produce a roughly equal miss in all of the curves. The cause of the misfits may be due to inaccuracies in the data caused by the weakness of the He^{++} beam, which was

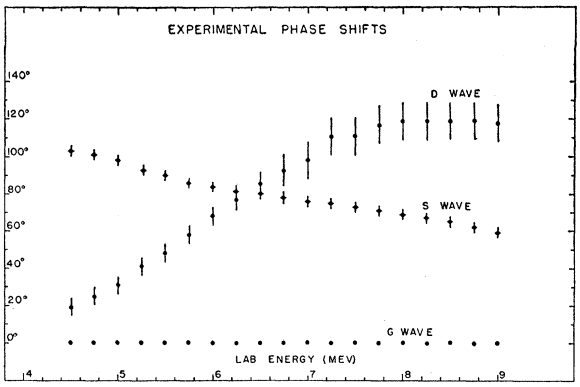

FIG. 3. Alpha-alpha scattering phase shifts derived from the present experiments, in degrees, plotted as a function of laboratory energy.

typically about 5×10^{-3} microampere. The phase shifts derived in this way are shown in Fig. 3. It should be noted that in this energy range δ_4 is identically equal to zero. The theoretical fits to the excitation curves calculated from these phase shifts are shown in Fig. 1.

An estimate of the errors to be associated with the phase shifts was made in the following way. By a series of cross-section calculations at 1-Mev intervals, it was determined how much variation in the S-wave phase shift was necessary to produce a 54° 44′ cross section which deviated from the cross section predicted by the derived phase shift by more than the experimental error associated with the experimental cross section at that energy. This deviation was called the "basic" error in the S-wave phase shift. This basic error was ±1° for the entire energy range. This procedure was then repeated for the D-wave phase shift at 1-Mev intervals for each integral value of the S-wave phase shift lying within the basic error. In this second series of calculations, however, the results were compared with the 30° 33′ and 70° 7′ cross-section predictions of the derived phase shifts. In this way, a basic error for the D-wave phase shift was established. This proved to be approximately ±1.5° at 5 and 6 Mev, and ±3° at 7, 8, and 9 Mev. To obtain a final estimate of the phase-shift errors, it was found necessary to multiply these basic errors by a factor of 3 in consideration of the poor fits to the data produced by the derived phase shifts.

The phase shifts derived in the present work are shown in conjunction with those derived by Heydenburg and Temmer, Russell *et al.*, and Nilson *et al.* in Fig. 4. As can be seen, the D-wave phase shift shows a typical resonant behavior near a laboratory energy of 6 Mev. Likewise, the beginning of a typical resonant behavior is also seen in the G-wave phase shift. The S-wave phase shift is presumed to rise very rapidly to 180° at an energy corresponding to the very narrow ground state and, as can be seen, decreases monotonically, passing through zero at approximately 20 Mev.

It will also be noticed from Fig. 4 that the S- and

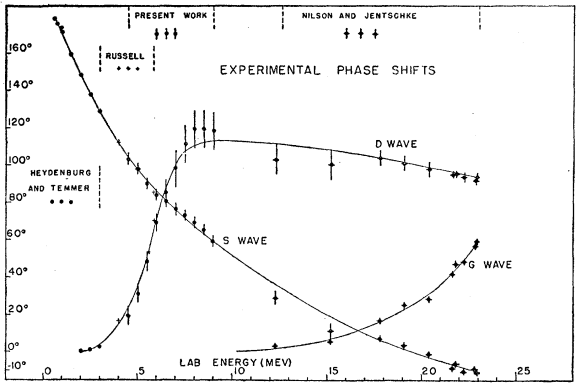

FIG. 4. Alpha-alpha scattering phase shifts derived in the present work are shown with those derived by Heydenburg and Temmer, Russell *et al.*, and Nilson *et al.* The phase shifts are shown in degrees plotted as a function of laboratory energy. Arbitrary smooth curves have been drawn through the data points.

D-wave phase shifts of Nilson *et al.* at the laboratory energies 12.3 Mev and 15.2 Mev do not seem to agree with a smooth curve drawn through the other *S*- and *D*-wave phase shift data points. In an attempt to understand this discrepancy, the angular distributions of Nilson *et al.* at these two energies were re-analyzed with the technique described above. The re-analysis yielded essentially the same phase shifts as reported by Nilson *et al.*

In addition two angular distributions were calculated from assumed phase shifts. The first of these angular distributions was calculated for a laboratory energy of 8 Mev with phase shifts which are compatible extrapolations of the derived phase shifts of Nilson *et al.* This angular distribution is shown in Fig. 5, with experimental points from the present work. The second angular distribution was calculated for a laboratory energy of 12.3 Mev using phase shifts that are reasonable extrapolations of the phase shifts derived from the present work. This angular distribution is shown in Fig. 6 with the experimental points of Nilson *et al.* Examination of these two figures shows that there is not much difference between the angular distributions calculated from the assumed phases and the experimental points. This in turn indicates that the cross section is not a strongly varying function of the phase

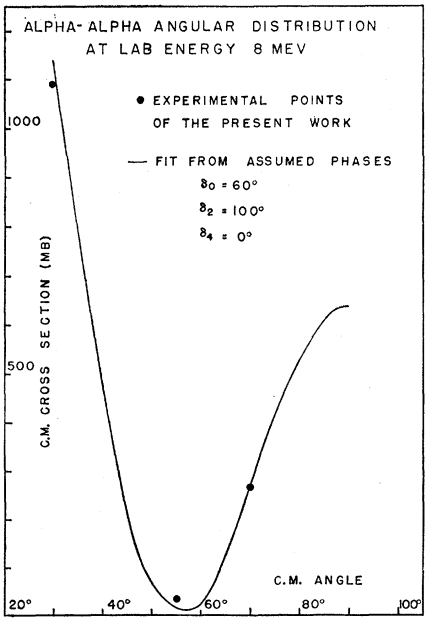

FIG. 5. Alpha-alpha angular distribution at a laboratory energy of 8 Mev calculated with phase shifts compatible with extrapolations of those derived by Nilson *et al.* Also shown are experimental data points from the present work. The cross section and angles are expressed in the center-of-mass system.

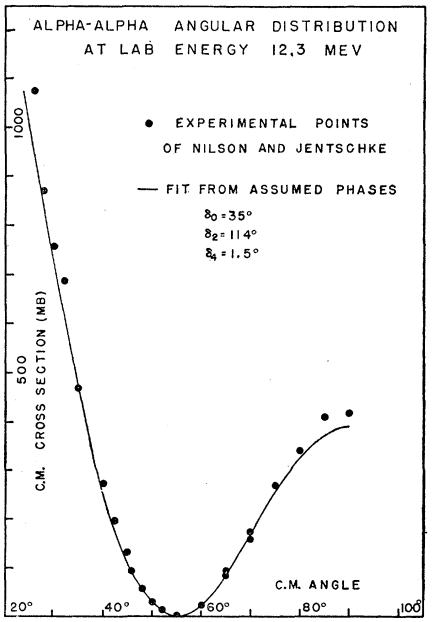

FIG. 6. Alpha-alpha angular distribution at a laboratory energy of 12.3 Mev calculated with phase shifts compatible with extrapolations of those derived in the present work. Also shown are experimental data points of Nilson *et al.* The cross section and angles are expressed in the center-of-mass system.

shifts in this energy region. It thus appears that more accurate cross-section measurements will have to be made before it can be decided whether the phase shifts extracted in the present work or those of Nilson and Jentschke more accurately represent the true phases. In any case the disagreement is not large.

SINGLE LEVEL DISPERSION THEORY ANALYSIS

In order to extract level parameters for the *D* state, the single level dispersion theory of Wigner and Eisenbud[13] was used to fit the *D*-wave resonance.

The nuclear phase shift δ_L can be expressed in terms of the dispersion theory in the following form:

$$\delta_L=\delta_{\lambda,R}-\phi_L, \quad \phi_L=\tan^{-1}[F_L/G_L]_{\rho=kR},$$

[13] E. P. Wigner and L. Eisenbud, Phys. Rev. **72**, 29 (1947).

where

$$\delta_{\lambda,R}=\tan^{-1}\frac{\frac{1}{2}\Gamma_{\lambda,L}}{E_{\lambda L}+\Delta_{\lambda L}-E_{\text{c.m.}}},$$

$$\tfrac{1}{2}\Gamma_{\lambda L}=[\rho\gamma_\lambda^2/A_L^2]_{\rho=kR},\quad A_L^2=F_L^2+G_L^2,$$

$$\Delta_{\lambda,L}=-\gamma_\lambda^2[g_L+L]_{\rho=kR},$$

and

$$g_L=\rho\left[\frac{1}{F_L}\frac{\partial F_L}{\partial\rho}-\frac{1}{A_L^2}\frac{G_L}{F_L}\right]_{\rho=kR}.$$

In these expressions, $E_{\text{c.m.}}$ = energy of the center-of-mass system, Mev, $E_{\lambda L}$ = constant expansion parameter, Mev, F_L = regular Coulomb wave function, G_L = irregular Coulomb wave function, $\rho=kr$, k = wave number $=\sqrt{2}(\mu E_{\text{c.m.}}/\hbar^2)^{\frac{1}{2}}$, R = nuclear radius in cm, γ_λ^2 = center-of-mass reduced width (constant) in Mev, $\Gamma_{\lambda,L}$ = center-of-mass laboratory width, Mev, ϕ_L = hard-sphere phase shift, and $\delta_{\lambda,R}$ = resonant phase shift. The resonance energy E_s is defined as that energy where $\delta_{\lambda,R}=90°$.

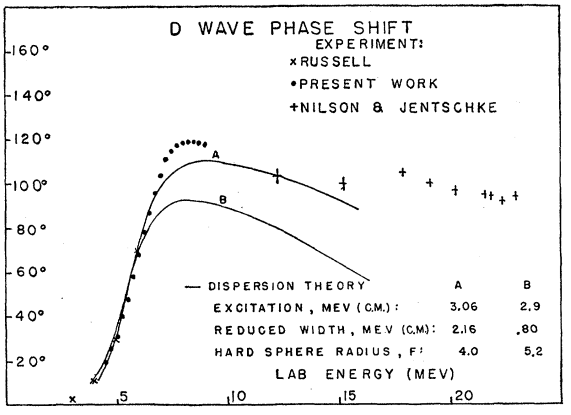

FIG. 7. Dispersion theory fits to variation of the D-wave phase shift *versus* laboratory energy. The points representing the phase shifts of the present work are taken from a smooth curve drawn through the actual derived phase shifts shown in Fig. 3. Note that there is good agreement between fit B and the experimental phase shifts at laboratory energies below 6 Mev.

The D-wave phase shift was calculated as a function of energy for various sets of parameters with the use of the Coulomb wave function tables of Bloch, Hull, Broyles, Bouricius, Freeman, and Breit.[14] Some of the poorer fits are shown in Fig. 7 and the best fit is shown in Fig. 8.

The parameters used in the best fit and the Wigner limit[15] for these parameters are given below.

Excitation in Be^8: 3.1 Mev (c.m.),

Reduced width: 3.5 Mev (c.m.),

Hard-sphere radius: 3.5×10^{-13} cm $\equiv$ 3.5 f,

[14] Bloch, Hull, Broyles, Bouricius, Freeman, and Breit, Revs. Modern Phys. **23**, 147 (1951).

[15] T. Teichmann and E. Wigner, Phys. Rev. **87**, 123 (1952).

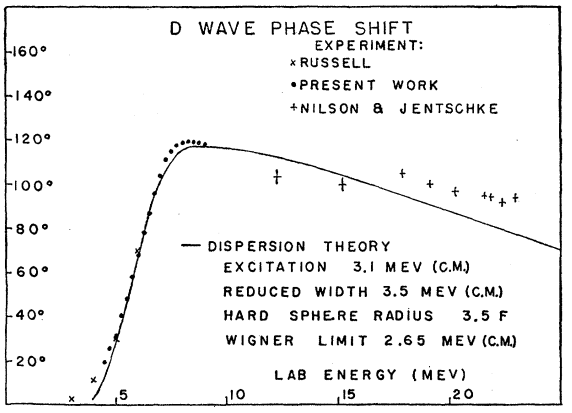

FIG. 8. The best dispersion theory fit to the D-wave phase shift variation *versus* laboratory energy. The points representing the phase shifts of the present work are taken from a smooth curve drawn through the actual derived phase shifts shown in Fig. 3.

$$\text{Wigner limit}=\frac{\frac{3}{2}\hbar^2}{\mu a^2}=2.65\text{ Mev (c.m.)},$$

$$\theta_\lambda^2=\gamma_\lambda^2\Big/\frac{\frac{3}{2}\hbar^2}{\mu a^2}=1.32.$$

The extreme width of the state in comparison with the Wigner limit, $3\hbar^2/2\mu a^2$, indicates that the D state in Be^8 is of almost wholly alpha-alpha parentage.

It is of interest to consider this calculation in the light of what is known about the alpha-alpha potential. Russell *et al.*[4] have shown that if the interaction between

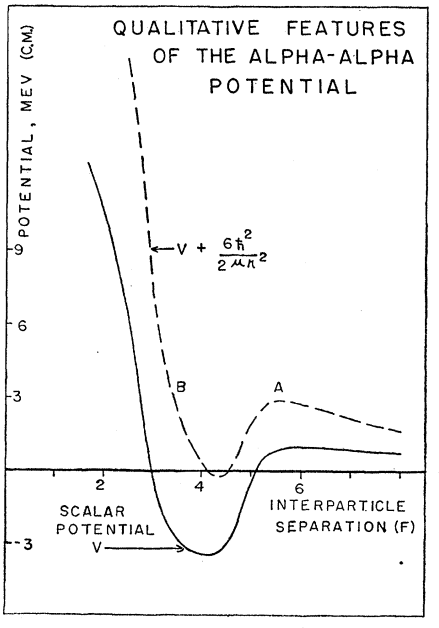

FIG. 9. Qualitative features of the alpha-alpha potential as derived by Russell *et al.* The potential is plotted in the center-of-mass system. The solid line represents the S-wave potential while the dashed line represents the D-wave potential.

two alpha particles can be described by a scalar potential and if the Be^8 nucleus is considered to be composed of two alpha particles at low excitation energies, this scalar potential will have the quantitative shape shown in Fig. 9. Since we are considering an interaction with nonzero angular momentum, a centrifugal potential term, $l(l+1)\hbar^2/2\mu r^2$, must be added to this potential. The sum of the scalar and centrifugal potentials, for $l=2$, is indicated by the dotted line. Now it will be noticed that the dispersion theory fit requires a hard-sphere radius which is quite small. In particular, the dispersion theory fit yields a hard-sphere radius of 3.5 f[1 fermi(f)$\equiv 10^{-13}$ cm], while Russell's arguments based on the D-wave phase shift at lower energies would indicate a hard-sphere radius of approximately 5.5 f. A possible explanation for this discrepancy is that at higher energies some of the hard-sphere scattering does not occur at point A but rather at point B (see Fig. 9), and thus the dispersion theory fit yields a radius which approaches the radius of the hard core at higher energies of bombardment. This argument is supported by the fact that the low-energy D-wave phase shift (with $E_{\text{lab}}\leq 6$ Mev) is fitted very well with a radius of 5.2 f (see Fig. 7). As the energy increases, a smaller radius must be used to fit the phase shift (see Fig. 8). These arguments indicate that the dispersion theory calculations are compatible with a repulsive core, scalar, alpha-alpha potential.

It should be noted that the Wigner limit is also altered from the usual definition by this potential. The Wigner limit may be thought of as the uncertainty in energy due to the confinement of the nuclear system within a specific volume (defined by R). Since there is a hard core to this potential, the system is more or less confined to a spherical shell of outer radius A and inner radius B so that the uncertainty in energy is greater than if the system were confined in a sphere of radius A.

DISCUSSION

As has been indicated before, the experimental phase shifts indicate only three states in Be^8 at excitation energies below 12 Mev; a 0^+ ground state at approximately 190-kev bombarding energy, a 2^+ state at approximately 3 Mev in Be^8, and a 4^+ state at approximately 11 Mev in Be^8. Unfortunately, this level structure is predicted by both the shell model[16] and the alpha-particle model.[17] However, the extreme widths of these states indicate that they are alpha-particle states and lend credence to the latter model.

With regard to the alpha-alpha potential, very interesting calculations have been performed by Humphrey[18] in which he has attempted to fit the experimental phase shifts with a Margenau potential[19] given by

$$\begin{aligned} V(r) &= \infty, \quad r<r_1 \\ &= -V_0, \quad r_1<r<r_0 \\ &= 4e^2/r, \quad r_0<r, \end{aligned}$$

and a Haefner potential,[17] given by

$$\begin{aligned} V(r) &= -D+\hbar^2q^2/2\mu r^2, \quad r<r_0 \\ &= 4e^2/r, \quad r>r_0. \end{aligned}$$

Quite good fits were obtained with the Haefner potential but, unfortunately, these fits were obtained by using different values of D for different values of l. He was unable to find one potential of this form which would fit all the phase shifts. It is hoped that work of this nature can be continued with more sophisticated potentials.

It appears there is a need for a type of dispersion theory which would be more suitable for hard core potentials. In terms of Fig. 9, such a theory might consider the hard sphere scattering as composed of two parts. A certain fraction, f, of the hard-sphere scattering would occur at radius B, while the rest of the hard sphere scattering would occur at radius A. This viewpoint, however, presents two difficulties. The first is that the fraction f would be a sensitive and probably complicated function of energy. The second problem is the effect of the potential between A and B on the hard-sphere scattering at B. A simple solution to these problems is not evident.

ACKNOWLEDGMENT

We wish to express our appreciation to The Shell Development Company, who generously made available the use of their IBM-650 computer.

[16] D. Kurath, Phys. Rev. **101**, 216 (1956).
[17] R. Haefner, Revs. Modern Phys. **23**, 228 (1951).
[18] C. Humphrey (private communication).
[19] H. Margenau, Phys. Rev. **59**, 37 (1941).